

# MTXPK.org: A Clinical Decision Support Tool Evaluating High-Dose Methotrexate Pharmacokinetics to Inform Post-Infusion Care and Use of Glucarpidase

Zachary L. Taylor<sup>1,2,3</sup> , Tomoyuki Mizuno<sup>3,4</sup> , Nieko C. Punt<sup>5</sup> , Balaji Baskaran<sup>6</sup>, Adriana Navarro Sainz<sup>6</sup> , William Shuman<sup>6</sup> , Nicholas Felicelli<sup>6</sup> , Alexander A. Vinks<sup>2,3,4</sup> , Jesper Heldrup<sup>7</sup>  and Laura B. Ramsey<sup>2,3,4,\*</sup> 

Methotrexate (MTX), an antifolate, is administered at high doses to treat malignancies in children and adults. However, there is considerable interpatient variability in clearance of high-dose (HD) MTX. Patients with delayed clearance are at an increased risk for severe nephrotoxicity and life-threatening systemic MTX exposure. Glucarpidase is a rescue agent for severe MTX toxicity that reduces plasma MTX levels via hydrolysis of MTX into inactive metabolites, but is only indicated when MTX concentrations are > 2 SDs above the mean excretion curve specific for the given dose together with a significant creatinine increase (> 50%). Appropriate administration of glucarpidase is challenging due to the ambiguity in the labeled indication. A recent consensus guideline was published with an algorithm to provide clarity in when to administer glucarpidase, yet clinical interpretation of laboratory results that do not directly correspond to the algorithm prove to be a limitation of its use. The goal of our study was to develop a clinical decision support tool to optimize the administration of glucarpidase for patients receiving HD MTX. Here, we describe the development of a novel 3-compartment MTX population pharmacokinetic (PK) model using 31,672 MTX plasma concentrations from 772 pediatric patients receiving HD MTX for the treatment of acute lymphoblastic leukemia and its integration into the online clinical decision support tool, MTXPK.org. This web-based tool has the functionality to utilize individualized demographics, serum creatinine, and real-time drug concentrations to predict the elimination profile and facilitate model-informed administration of glucarpidase.

## Study Highlights

### WHAT IS THE CURRENT KNOWLEDGE ON THE TOPIC?

☑ Currently, both the glucarpidase drug label and glucarpidase consensus guideline are available to guide the clinical use of glucarpidase for patients with life-threatening methotrexate (MTX) toxicity, but there are challenges to interpretation and implementation in the clinical setting.

### WHAT QUESTION DID THIS STUDY ADDRESS?

☑ The study aimed to address the questions, “How can we facilitate the understanding of when glucarpidase is indicated for patients receiving high-dose (HD) MTX?” and “Can we develop a population pharmacokinetic (PK) model-informed

decision platform that adequately describes the MTX PK in patients with delayed clearance?”

### WHAT DOES THIS STUDY ADD TO OUR KNOWLEDGE?

☑ MTXPK.org, a free, online clinical decision support tool now exists to facilitate the understanding of when glucarpidase is indicated for patients receiving HD MTX.

### HOW MIGHT THIS CHANGE CLINICAL PHARMACOLOGY OR TRANSLATIONAL SCIENCE?

☑ This tool will facilitate clinical decisions by clinical pharmacists and oncologists in when to administer glucarpidase, and provides an estimate of when the patient may reach the MTX concentration threshold for discharge.

<sup>1</sup>Department of Molecular, Cellular, and Biochemical Pharmacology, University of Cincinnati, Cincinnati, Ohio, USA; <sup>2</sup>Division of Research in Patient Services, Cincinnati Children's Hospital Medical Center, Cincinnati, Ohio, USA; <sup>3</sup>Division of Clinical Pharmacology, Cincinnati Children's Hospital Medical Center, Cincinnati, Ohio, USA; <sup>4</sup>Department of Pediatrics, University of Cincinnati, Cincinnati, Ohio, USA; <sup>5</sup>Medimatics, Maastricht, The Netherlands; <sup>6</sup>Division of Biomedical Informatics, Cincinnati Children's Hospital Medical Center, Cincinnati, Ohio, USA; <sup>7</sup>Childhood Cancer and Research Unit, University Children's Hospital, Lund, Sweden. \*Correspondence: Laura B. Ramsey ([laura.ramsey@cchmc.org](mailto:laura.ramsey@cchmc.org))

Received March 2, 2020; accepted June 3, 2020. doi:10.1002/cpt.1957

Methotrexate (MTX) is a commonly used antifolate administered intravenously at high doses to effectively treat pediatric and adult patients with acute lymphoblastic leukemia (ALL), osteosarcoma (OS), and lymphoma.<sup>1–4</sup> Unfortunately, patients receiving i.v. high-dose (HD) MTX often experience significant toxicities of the kidneys and eventually the liver and gastrointestinal tract. To reduce these toxicities, supportive care (including folate supplementation, fluid hyper hydration, and urine alkalization before and during the MTX treatment) is used to facilitate renal elimination.<sup>5</sup> However, there is still considerable interpatient variability in clearance of HD MTX with severe delayed MTX clearance seen in 0.5–1% of pediatric patients with ALL,<sup>6,7</sup> 1.8% of courses of 12 g/m<sup>2</sup> over 4 hours in youths with OS,<sup>4</sup> and 1–12% of adults treated for lymphoma.<sup>8,9</sup> Patients with delayed MTX clearance are at an increased risk for severe nephrotoxicity, which further reduces MTX elimination and can culminate in life-threatening systemic MTX exposure.

Currently, there is a lack of clinical tools for the identification of patients likely to experience delayed MTX clearance prior to the initiation of treatment or early after the infusion. As a result, response to patients with delayed MTX clearance tends to be reactive. Once concentrations rise above critical limits, rescue by folinic acid can be inadequate.<sup>7</sup> In such cases, glucarpidase, a US Food and Drug Administration (FDA)-approved exogenous enzyme, is administered as a rescue agent that rapidly hydrolyzes MTX into two inactive metabolites that are eliminated via renal and nonrenal pathways.<sup>6,10–13</sup> The rapid hydrolysis by glucarpidase reduces plasma MTX concentrations by > 90% within 15 minutes of administration.<sup>4,14–17</sup> Glucarpidase is only indicated when MTX concentrations are > 2 SDs above the mean excretion curve specific for the given dose<sup>10</sup> in order to avoid underexposure to MTX and risk of relapse. Appropriate interpretation of the indication and administration of glucarpidase remains a challenge because many clinicians do not know the expected excretion curve and two times SD. As a result, a recent glucarpidase consensus guideline was published in an attempt to clarify the interpretation of the glucarpidase indication by providing a glucarpidase treatment algorithm that detailed MTX concentrations at select time points following a MTX infusion of several common dosing regimens.<sup>11</sup> Although beneficial, the clinical interpretation of MTX concentrations that do not correspond to the algorithm's time points prove to be a limitation of its use.

Therefore, the purpose of this study was to develop a web-based clinical decision support tool that provides an MTX population pharmacokinetic (PK) model-informed interpretation in tandem with the glucarpidase consensus guideline to facilitate the administration of glucarpidase in all patients receiving HD MTX, regardless of indication or age. Our aim was to develop a novel MTX population PK model using PK data from the Nordic Society for Pediatric Hematology and Oncology (NOPHO) and evaluate it as a model for the web-based clinical decision support tool, MTXPK.org. Although several PK models for HD MTX have been described, they may not describe patients with delayed clearance well because they are constructed from MTX concentrations only up to 44 hours after the start of MTX infusion.<sup>18–23</sup> We hypothesize that our NOPHO PK model will better fit patients with delayed MTX

clearance than currently available population PK models due to the dense PK sampling from patients with delayed MTX clearance with concentrations recorded up to 300 hours after the start of infusion.

## METHODS

### Study design

This study retrospectively analyzed PK data from 820 deidentified pediatric patients who were receiving HD MTX for the treatment of Philadelphia chromosome-negative ALL between January 2002 and December 2014. Included in the current study were children (ages 1–18.83 years at diagnosis) from hospitals across Denmark, Finland, Lithuania, Norway, and Sweden receiving treatment in accordance with the NOPHO ALL2000 and ALL2008 protocols.<sup>2,3,7</sup> Patients were not included if they received glucarpidase because the immunoassay measurements of MTX have interference from the DAMPA that results after MTX is cleaved by glucarpidase.<sup>11</sup> Forty-eight patients and 679 concentrations were excluded from the PK analysis due to missing dosing information. In brief, patients were scheduled to receive 6–8 courses of i.v. HD MTX (5 or 8 g/m<sup>2</sup>) over a 24-hour infusion with folinic acid rescue occurring at 36 or 42 hours after the start of infusion. Serial plasma MTX levels were collected at 24, 36, and every 6 hours after the start of infusion until the plasma concentrations reached  $\leq 0.2 \mu\text{mol/L}$ .<sup>7</sup> MTX concentrations in plasma were quantified using one of two comparable immunoassay methods: enzyme-multiplied immunoassay technique or fluorescence polarization immunoassay.<sup>7,24</sup> Clinical covariates, like serum creatinine (SCr) levels were recorded prior to the start of each MTX infusion and at least daily in tandem with plasma MTX levels. Demographic covariates, such as age, sex, body surface area (BSA), weight, and country of treatment, were also included in the database. The NOPHO ALL2000 and ALL2008 protocols were approved by the Ethical Committee of the Capital Region of Denmark and by local ethical review boards.

### Model development and Bayesian estimation

We performed a population PK analysis of HD MTX using nonlinear mixed-effects modeling implemented in NONMEM version 7.2.0 (ICON, Ellicott City, MD) and validated using KinPop++. Two-compartment and three-compartment structural models were considered. PK data was assumed to be log-normally distributed.<sup>25</sup> The three-compartment with an exponential residual error model was chosen as the base model after considering objective function value (OFV) and goodness-of-fit plots. Clinical (SCr) and demographic (BSA, weight, age, and sex) data collected during the course of the MTX treatment were included in the covariate analysis. Additional information regarding the development of the population PK model can be found in the **Supplementary Material S1**. A module for Bayesian estimation was included in the MTXPK.org platform using a three-compartment structure model developed using the visual PK/pharmacodynamic (PD) model designer Edsim++ (Mediware, Prague, Czech Republic) and executed using an Edsim++ compatible PK/PD modeling engine.<sup>26,27</sup>

### Evaluation of MTX population PK models

Two published MTX population PK models,<sup>18,28</sup> and our three-compartment MTX model were tested in an MTXPK.org prototype (MTXSim), which uses the same platform libraries as MTXPK.org. Model parameters and rationale for selection are detailed in the **Table S1**.<sup>18,28</sup> These models were evaluated on their prediction bias and prediction precision using a small validation cohort of pediatric and young adult patients with ALL, lymphoma, and OS and whose data were not part of the modeling set.<sup>29</sup>

### Integration into a web-based clinical decision support tool

At the top level is the web application (**Figure S1**). It was created so that it could run on both large and small screen devices by utilizing responsive

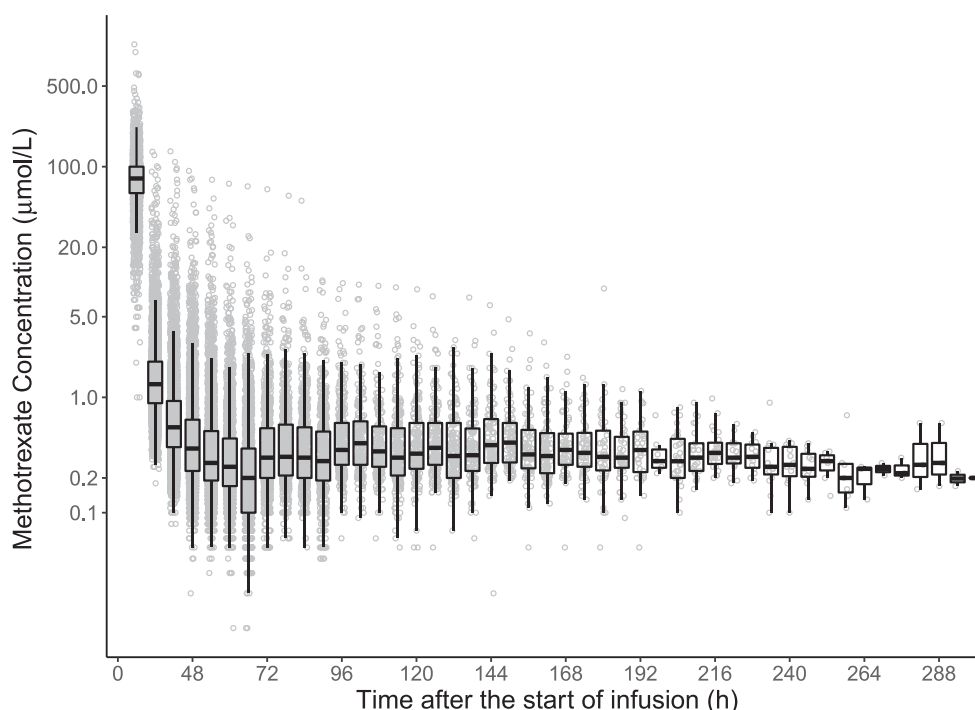


**Figure 1** Concentration-time plot of the Nordic Society for Pediatric Hematology and Oncology dataset. Individual concentrations are in blue with a box and whiskers plot shown on top. The black line represents the median value. The box plot illustrates the interquartiles with the whiskers representing the two SDs.

web design. The application presents different design elements based on the user's screen size and platform. It was built with React, a JavaScript library, and uses a Web API, to send data to and receive data from a library containing all MTX-specific business logic (BSA calculator and dosing schedules for each indication). This MTX-specific library uses a general purpose PK/PD modeling engine for simulation and Bayesian estimation, which, in turn, uses models from a PK/PD model repository.<sup>27</sup> MTX models were designed, executed, and validated using Edsim++ 1.80 (Mediware).<sup>26</sup> The PK/PD modeling engine runtime is capable of executing these models outside Edsim++. A stand-alone windows application (MtxSim) was used for end-to-end validation of the system (including the models) and as a prototype tool for the web development team building MtxPK.org. In MtxSim, different models can be selected for testing.

### Statistics

Comparative statistical analysis between sex and country included the Student's *t*-test and one-way analysis of variance, respectively (mean  $\pm$  SD). A  $P < 0.05$  was considered statistically significant. Linear regression was used to determine the  $R^2$  for the goodness-of-fit plots. Statistical analysis was completed using GraphPad Prism 8.0.1.

## RESULTS

### Population PK model development

The final population PK model was based on data from 772 patients, covering 4,986 courses, and 31,672 plasma MTX concentrations (**Figure 1**)—with 5,535 concentrations recorded  $\geq 96$  hours after the start of infusion. The demographic and PK information for the NOPHO dataset is summarized in **Table 1**. A three-compartment model using an exponential residual error model best described the PK of HD MTX in Nordic pediatric patients with ALL (**Figure 2**). The OFV for the base

three-compartment model was significantly lower than that for the base two-compartment model ( $\Delta\text{OFV} = -6,136.43$ ,  $P < 0.001$ ), suggesting that the three-compartment model provided significantly improved description of the data.<sup>30</sup> The three-compartment model also demonstrated significant improvement in the population prediction performance (**Figure 2a**) compared with the two-compartment model (**Figure 2b**,  $P < 0.001$ ), the latter was prone to substantial model-based overestimation of low MTX concentrations and MTX clearance. The three-compartment model demonstrated less error as the time after the dose increased (**Figure 2c**) compared with the two-compartment model (**Figure 2d**). Additional analysis of the residuals using the root mean square error as a

**Table 1** Patient demographics

	Median, <i>n</i>	Range (%)
Age, years	4	(1–18.83)
Body surface area, m <sup>2</sup>	0.745	(0.4–2.31)
Courses per patient	8	(1–8)
Country		
Denmark	207	(27%)
Finland	78	(10%)
Norway	59	(8%)
Sweden	428	(55%)
Dose, g/m <sup>2</sup>	5	(0.6–10.1)
Sex, female	333	(43%)
Serum creatinine, µmol/L	29	(4–155)
Weight, kg	17.8	(7.2–105)

measure of model accuracy revealed a 44% reduction in the unexplained variance while using the three-compartment model, further demonstrating that the three-compartment structural model outperforms the two-compartment model.

### Covariate model

The stepwise inclusion of covariates is presented in **Table 2**. Among the clinical and demographic covariates considered, the patient's

BSA yielded the largest reduction in OFV ( $\Delta\text{OFV} = -2,358.81$ ,  $P < 0.001$ ) and displayed a better coefficient of determination with clearance (**Figure 3a**,  $R^2 = 0.54$ ) than the patient's body weight (**Figure 3b**,  $R^2 = 0.36$ ). Weight-based and BSA-based allometrically scaled models were evaluated (details in the **Supplementary Material S1**). All PK parameters (CL, V1, Q2, V2, Q3, and V3) were normalized to a BSA of  $1.73 \text{ m}^2$  because the OFV was decreased by 2,605.79 compared with a model that only normalized CL to BSA (**Table 2**). After the clearance was normalized,

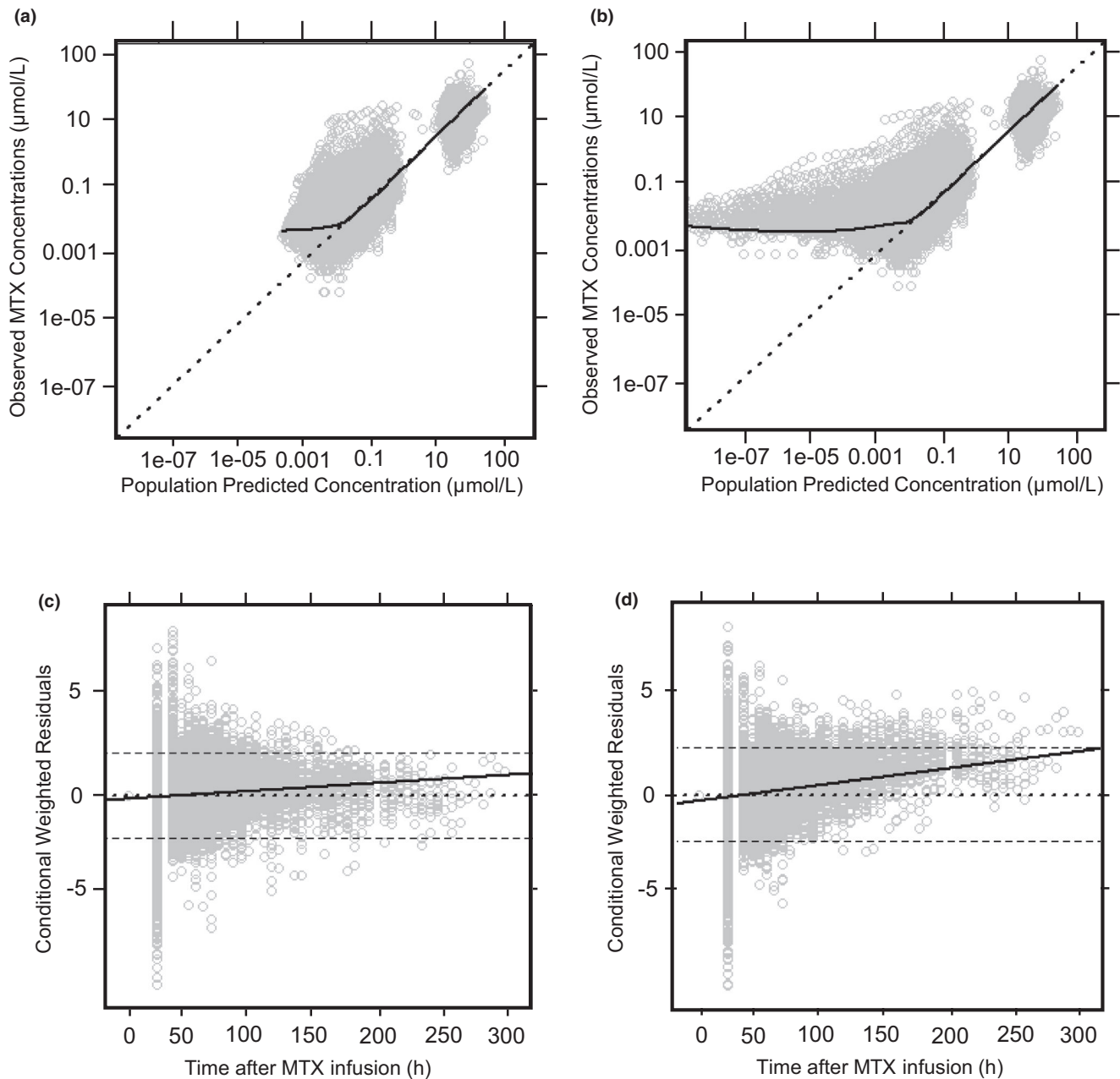


**Figure 2** Comparing the goodness-of-fit plots for two-compartment and three-compartment structural models. The three-compartment model showed significantly less bias at lower predicted concentrations (**a**) compared to the two-compartment model (**b**), which displayed overestimation of clearance. The three-compartment model displayed improved predictive performance at later times following a methotrexate (MTX) infusion (**c**) compared with the two-compartment model (**d**). A total of 1,494 weighted residuals (4.7%) were found outside of  $\pm 2$  conditional weighted residuals (CWRES). The CWRES displayed a normal distribution with 649 residuals below  $-2$ . For **a** and **b**, the dotted line represents the line of identity. For **c** and **d**, the dotted line represents the zero-line. The dashed lines represent the two SDs. The solid black line represents the trend line for all figures.

**Table 2** Forward stepwise inclusion of covariates

No.	Covariates	Parameter(s)	Covariate model	$\Delta$ OFV	$P < 0.05$	Reference model	Notes
1	Base Model	–	–	–	–	–	3-CP, i.v., linear elimination
2	BSA	All	Normalize	–2,358.81	Yes	1	Normalized to 1.73 m <sup>2</sup>
3	Weight	All	Normalize	–1,260.02	Yes	1	Normalized to 70 kg
4	SCr	CL	Power	–39.59	Yes	1	(SCr/29) <sup>power</sup>
5	BSA + SCr	All + CL	Power	–702.73	Yes	2	Normalization + (SCr/29) <sup>power</sup>

$\Delta$ OFV, change in the objective function value; BSA, body surface area; CL, clearance; CP, compartment; No., model number; SCr, serum creatinine.

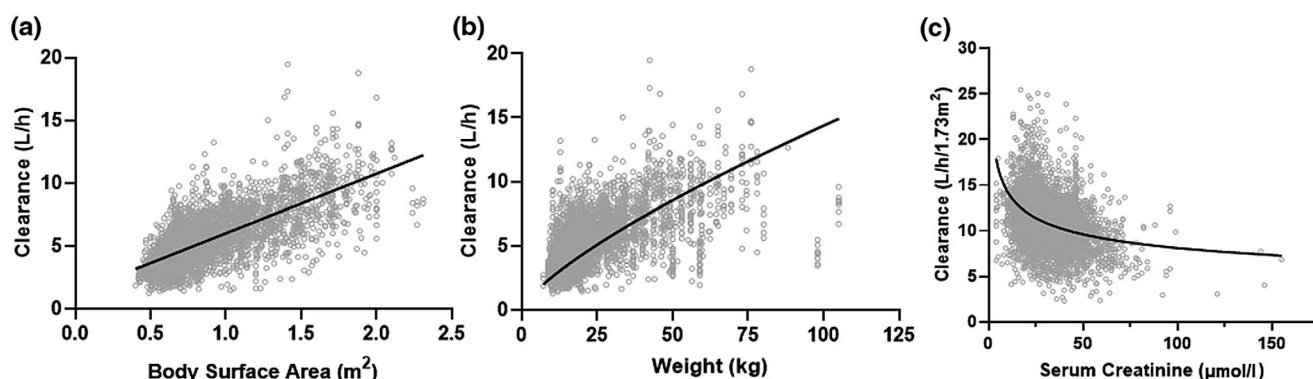


**Figure 3** Covariate analysis. The coefficient of determination for body surface area (BSA) and the estimated clearance (**a**,  $R^2 = 0.54$ ) is a stronger relationship than the coefficient of determination for weight allometrically scaled to 70 kg and the estimated clearance (**b**,  $R^2 = 0.25$ ). Serum creatinine demonstrated a nonlinear with clearance normalized to BSA (**c**). The gray dots represent clearance estimates at the first serum creatinine level for each patient course.

demographic covariates, such as age and sex, did not significantly improve clearance estimates (**Figure S2**). Finnish patients had an estimated 26% faster clearance compared with Swedish, Danish, and Norwegian patients (**Figure S3**). SCr was negatively correlated to normalized clearance (**Figure 3c**), which was accounted for by incorporating SCr as a time-varying covariate into a power component normalized to the population median of 29  $\mu\text{mol/L}$  (0.33 mg/dL). Once adjusted, SCr further explained interindividual variability in clearance and reduced the OFV by  $-702.73$  ( $P < 0.001$ ). The equation for the final covariate model is presented below:

$$CL_i = CL_{\text{pop}} * \left( \frac{BSA}{1.73} \right) * \left( \frac{SCR}{29} \right)^{-0.247}$$

The parameter estimates for the final model are presented in **Table 3**. Model estimates for the interindividual variability of V1 and Q2 approached zero and were therefore fixed parameters.<sup>30,31</sup> Model performance further improved once these parameters were fixed.

### Evaluation of MTX population PK models

Three models were implemented and tested as part of the MTXPK.org platform using the MTXSim prototype. Model parameters for each of the published population PK models are summarized in **Table S1**. The model parameters were integrated into the MTXSim prototype with Edsim++ PK engine functionality,<sup>26,27</sup> which enabled us to load patient data from a previously published cohort<sup>29</sup> onto each model to generate individual Bayesian estimated PK

estimations. Comparisons between PK estimates and observed values were made. The new three-compartment model demonstrated the least model bias and best model precision compared with other published models (**Table S2**). The three-compartment model performed well among several validation cohorts that included all ages and indications (**Table S3**).

### Web-based clinical decision support tool

The three-compartment model was selected as the default MTX population PK model to be integrated into the MTXPK.org webtool. This online, free-to-use tool allows the user to enter patient data that can be locally saved and reloaded later to add more information; however, nothing is stored by the website. The user will begin by entering the patient's demographics, disease indication, and treatment regimen (**Figure 4a**) followed by the patient's plasma MTX concentrations and SCr concentrations (**Figure 4b**). Once finished, the user can generate the individual's personalized concentration-time curve, "Time to Elimination Threshold," and estimated area under the elimination curve (AUC; **Figure 4c**). The user can immediately visually compare the patient's elimination curve to that of the population average, the consensus guideline thresholds, and the 2 SD greater than the mean elimination curve described in the glucarpidase label. The user is provided with quantitative metrics as well; when the cursor hovers over the concentration-time curve, estimated plasma MTX concentration values are provided with the population average and 2 SD estimates for the same time point. In the case of our example patient, which

**Table 3 Final model parameter estimates**

Parameters	Mean	Relative standard error (%)	Interindividual variability	Relative standard error (%)
CL, L/h/1.73 m <sup>2</sup>	11	0.7	0.08	4.7
V1, L/1.73 m <sup>2</sup>	16.5	5.2	0 FIX	–
Q2, L/h/1.73 m <sup>2</sup>	0.602	4.1	0 FIX	–
V2, L/1.73 m <sup>2</sup>	4.55	3.4	0.12	4.3
Q3, L/h/1.73 m <sup>2</sup>	0.111	2	0.13	6.7
V3, L/1.73 m <sup>2</sup>	13.1	5	0.10	14.4
SCr	–0.247	5.7	–	–

CL, clearance of methotrexate from the central compartment; Q2, inter-compartmental clearance for vascular peripheral compartment; Q3, intercompartmental clearance for the nonvascular compartment; SCr, pharmacokinetic estimate for serum creatinine; V1, volume of distribution of methotrexate in the central compartment; V2, volume of distribution of methotrexate in the vascular compartment; V3, volume of distribution of methotrexate in the nonvascular compartment.

contains real PK data, the MTX concentration at 23 hours is higher than the actionable MTX concentrations outlined in the glucarpidase guideline and borderline on the glucarpidase drug label. Looking at the 36-hour time point, this patient is below the glucarpidase consensus guideline threshold, but remains higher than the glucarpidase label threshold. At hours 42 and 48, our example patient's plasma concentrations equal that of the actionable concentrations outlined in the glucarpidase consensus guideline. Following the glucarpidase drug label and consensus guideline, our example patient would fit the indication for glucarpidase administration. **Figure 4d** illustrates the full concentration-time curve of our example patient, which resembles that of the Bayesian estimated forecasting seen in **Figure 4c**. Furthermore, the user can also utilize the "Time to Elimination Threshold" and estimated AUC located in the top of the window for additional guidance. Last, the user has the capability to generate and print the patient's personalized PK report; this can be given to the patient's family, stored physically in a patient's file, or uploaded into the electronic health record for future reference.

## DISCUSSION

The purpose of this project was to develop a web-based clinical decision support tool that utilized an MTX population PK model and Bayesian estimation to facilitate optimal administration of glucarpidase for patients with delayed MTX clearance or high plasma MTX concentrations following an i.v. administration of HD MTX.

The current clinical challenges pertaining to optimal administration of glucarpidase arise when the time of a collected blood sample does not correspond to the time points outlined by the glucarpidase consensus guideline, appear very close to the consensus guideline's actionable concentrations, or reveal rapidly rising SCr concentrations. MTXPK.org is able to mitigate these clinical challenges by facilitating model-informed administration of glucarpidase through the use of population PK modeling and *a posteriori* Bayesian estimation. The web-based clinical decision support tool works by allowing the user to enter the patient's demographics, real-time drug concentrations, and SCr concentrations into the tool (**Figure 4a,b**). The tool then models the

individual's information and simulates a personalized elimination curve using Bayesian estimation (**Figure 4c**). MTXPK.org illustrates the average elimination curve for the population surrounded by the 2 SD greater than the mean elimination curve, described in the glucarpidase drug label,<sup>10</sup> and the actionable plasma MTX concentrations at specified time points, outlined in the glucarpidase guideline.<sup>11</sup> The clinician is provided with personalized visual and numeric information pertaining to their patient's MTX elimination curve that can be compared with the glucarpidase drug label and consensus guideline to facilitate model-informed decisions about postinfusion supportive care and the administration of glucarpidase.

A similar tool to MTXPK.org was launched by Barrett *et al.* at Children's Hospital of Philadelphia (CHOP) that integrated modeling and simulation into a hospital-based decision support tool to guide leucovorin rescue for patients receiving HD MTX.<sup>32</sup> The Barrett *et al.* MTX dashboard tool focused on the visualization of individualized elimination curves simulated from *a posteriori* Bayesian estimation of HD MTX. The elimination profile generated by the Barrett tool overlaid a leucovorin nomogram with additional dosing events relative to biomarkers of HD MTX toxicity presented to the clinician to guide dosing of MTX and rescue with leucovorin.<sup>33</sup> Commercial and institutional support tools are available; however, MTXPK.org is the only free, publicly available clinical decision support tool to inform postinfusion care following i.v. infusion of HD MTX.

In order to achieve optimal administration of glucarpidase, MTXPK.org needs to provide an accurate estimation of a patient's individualized elimination curve and the population mean  $\pm$  2 SD that corresponds to the glucarpidase label indication. The description of the average population elimination curve and associated 2 SD is captured in the default population PK model for MTXPK.org, which was developed using the extensive and PK-rich NOPHO database that included 5,535 plasma MTX concentrations collected > 96 hours from the start of infusion in 400 patients. Typical MTX population PK models are developed using PK data up to 44 hours after the start of infusion<sup>18–23</sup> or contain few samples from patients with delayed MTX clearance.<sup>28,34,35</sup> These models overestimate MTX clearance and plasma concentrations when used to evaluate patients with delayed MTX clearance (as illustrated by the NOPHO two-compartment model in **Figure 2b**).

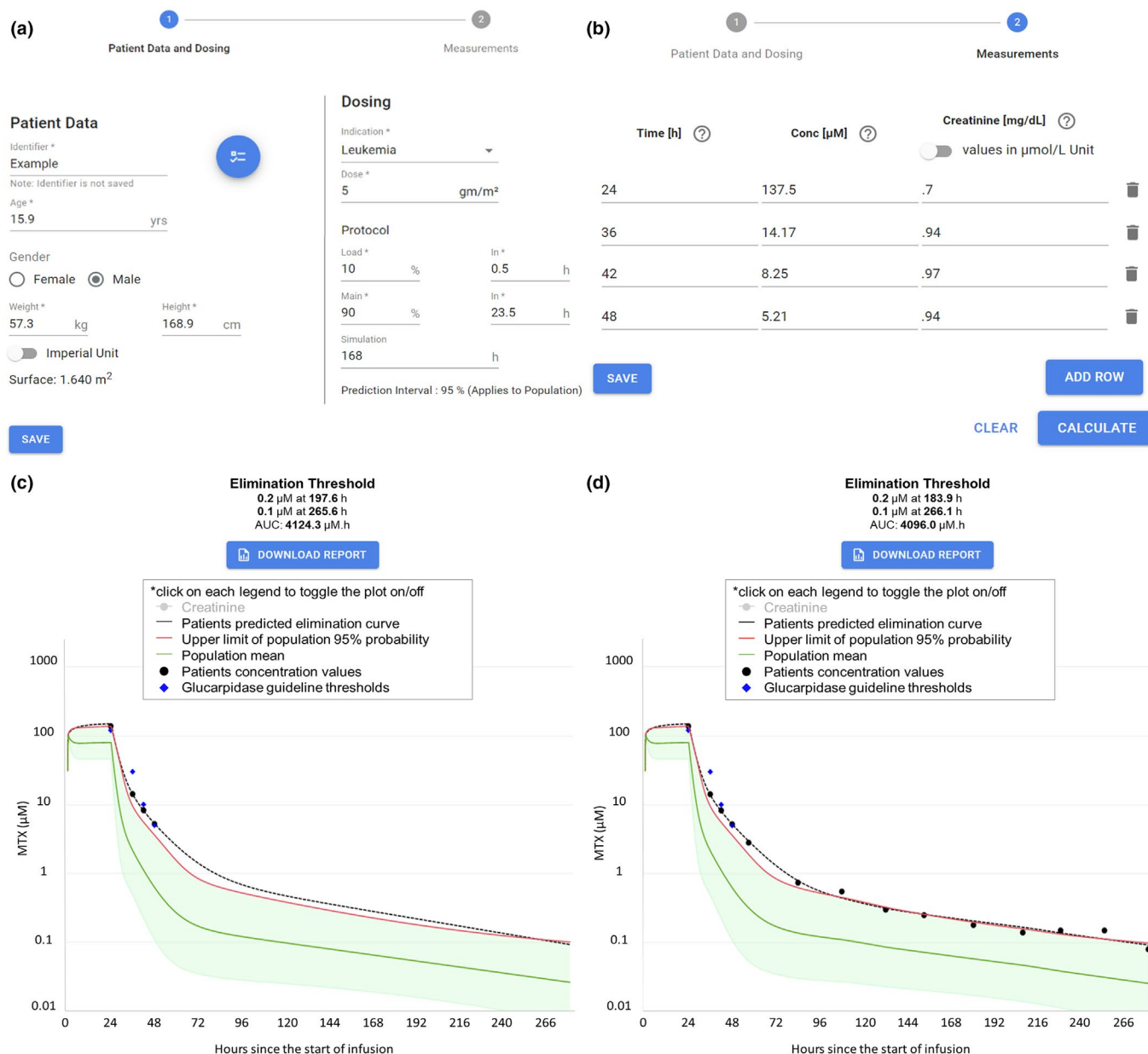


**Figure 4** Screenshots of MTXPK.org. **(a)** Patient demographics are easily loaded into the “Patient Data and Dosing” screen. Plasma methotrexate (MTX) concentrations and serum creatinine levels are added to the “Measurements” tab **(b)**. After hitting “Calculate,” the individualized pharmacokinetic (PK) estimates and concentration-time curve are generated **(c)**. With the use of MTXPK.org, the user would conclude that this patient would meet the indication for glucarpidase because the individualized PK elimination curve (black line) is higher than the elimination curve for the population (green line), the two SDs (red line), and is close to the concentrations outline by the glucarpidase guideline (purple diamonds). The full concentration-time curve for the example patient **(d)** demonstrates the accurate forecasting of plasma MTX concentrations. AUC, area under the elimination curve.

The three-compartment model provides a better estimation of the average elimination profile for the population and improved the description of the significant interpatient variability compared with the two-compartment model, which are critical for the accurate visualization and appropriate interpretation of the glucarpidase drug label. Physiologically, the third compartment might be able to reflect the redistribution of intracellular MTX, which is the site of action.<sup>36,37</sup> Thus, MTXPK.org uses a well-defined population PK model to generate the visual and numeric information associated

with the glucarpidase drug label and consensus guideline, which are used to facilitate the optimal administration of glucarpidase.

Aside from the accurate visualization of the glucarpidase label indication of 2 SD greater than the mean, MTXPK.org needs to accurately simulate a personalized elimination profile from the patient’s real-time drug concentrations and SCr concentrations using Bayesian estimation. The model parameters for the default population PK model for MTXPK.org serves as reliable, prior knowledge for *a posteriori* Bayesian estimation. This allows MTXPK.org to

accurately forecast plasma MTX concentrations for a given patient using the information provided to the tool, with more drug concentrations shown to improve Bayesian estimations through improved Bayesian learning<sup>33,38,39</sup> (Figure 4c,d). The three-compartment model provides more accurate forecasting of plasma MTX concentrations following the infusion of HD MTX than the two-compartment models we used. Utilizing Bayesian estimation has the potential to limit the amount of blood samples collected during postinfusion care and thus reducing the cost of care. Accurate Bayesian estimation also means that MTXPK.org has the capability to estimate the total MTX exposure by calculating the AUC. Estimated MTX AUC provides an additional metric to govern therapy; maintaining a target exposure could guide therapeutic outcomes while mitigating patient toxicity. Along with an estimated AUC, MTXPK.org is able to estimate the “Time to Elimination Threshold” in hours after the start of MTX infusion. This information can help establish expectations for appropriate inpatient duration and possibly reduce the financial costs to both the patient and institution.<sup>40</sup> Most importantly, MTXPK.org utilizes *a posteriori* Bayesian estimation to illustrate a patient’s individualized elimination curve from real-time drug concentrations that can be visually and numerically assessed by the clinician to facilitate model-informed administration of glucarpidase.

Despite this model’s attractive performance characteristics, there are some limitations to the model. It is unclear whether the model fit to a primarily European patient population can be generalized to patients of non-European descent, although in other studies that included a more diverse cohort, race explained little of the interindividual variability of MTX clearance.<sup>41</sup> Additionally, although the NOPHO database proved to be the richest MTX PK data available to us, the data were not able to support an estimation of the interindividual variability for the V1 and Q2 model parameters. This could impact the tool’s ability to accurately capture the early distribution phase in an elimination profile; however, clinicians are most likely to use the tool after the early phase, when they have measured the plasma MTX (for 24-hour infusions, clinical use would occur at 36 or 42 hours, and for 3–6-hour infusions, clinical use would occur at 24 hours). Additionally, the NOPHO database had limited covariates to explore. There is considerable interindividual variability in MTX clearance that previous publications have demonstrated to be partially explained by serum albumin,<sup>42</sup> creatinine clearance,<sup>40,43</sup> estimated glomerular filtration rate,<sup>28</sup> concomitant medications,<sup>44</sup> and *SLCO1B1* genotype.<sup>18,41,45,46</sup> Furthermore, our PK data did not include information regarding aspects of supportive care, like fluid hydration and urine pH, which can impact MTX clearance.<sup>35,47</sup> Future work will aim to evaluate the clinical success of MTXPK.org and attempt to expand on covariates that may improve the model’s predictive performance. Moreover, incorporating plasma MTX samples from delayed MTX clearance in patients after they have received glucarpidase into our default model will update MTXPK.org so that it can provide model-informed clinical care for these patients. Initial feedback from clinicians indicated that some would prefer it be included in the electronic health record to automatically pull in HD MTX dose, and MTX and SCr measurements, similar to the CHOP clinical decision support tool. Clinicians practicing at hospitals without an electronic medical record system have indicated that they

would gladly enter the data on the webtool and use it on every patient receiving HD MTX. Thus far, MTXPK.org has been used by > 900 unique users in at least 35 countries. As it stands, MTXPK.org is a free, web-based clinical decision support tool that can facilitate model-informed administration of glucarpidase for patients with delayed MTX clearance or high plasma MTX concentrations following the i.v. administration of HD MTX.

#### SUPPORTING INFORMATION

Supplementary information accompanies this paper on the *Clinical Pharmacology & Therapeutics* website ([www.cpt-journal.com](http://www.cpt-journal.com)).

#### ACKNOWLEDGMENTS

The authors are grateful to Maureen O’Brien and Jennifer Young for their guidance on the clinical utility of our decision support tool. We would like to thank all participating NOPHO institutions and physicians for their collection of MTX PK data used in this study. We appreciate Dr. Edmund Capparelli allowing us to test our model fit using data described in Kawakatsu *et al.*<sup>28</sup> Additionally, we are grateful to the patients and families who contributed their data to our study.

#### FUNDING

The development of the MTXPK.org webtool was supported by an unrestricted educational grant from BTG International.

#### CONFLICT OF INTEREST

L.B.R. and T.M. received research funding from BTG International. N.P. is president of Medimatics, a company that provides consulting services on medical information systems located in Maastricht, The Netherlands. All other authors declared no competing interests for this work. As an Associate Editor for *Clinical Pharmacology & Therapeutics*, Alexander A. Vinks was not involved in the review or decision process for this paper.

#### AUTHOR CONTRIBUTIONS

Z.L.T., T.M., N.C.P., B.B., A.N.S., W.S., N.F., A.A.V., J.H., and L.B.R. wrote the manuscript and designed the research. Z.L.T., T.M., N.C.P., A.A.V., J.H., and L.B.R. performed the research and analyzed the data.

© 2020 The Authors. *Clinical Pharmacology & Therapeutics* published by Wiley Periodicals LLC on behalf of American Society for Clinical Pharmacology and Therapeutics.

This is an open access article under the terms of the Creative Commons Attribution-NonCommercial License, which permits use, distribution and reproduction in any medium, provided the original work is properly cited and is not used for commercial purposes.

- Jolivet, J., Cowan, K.H., Curt, G.A., Clendeninn, N.J. & Chabner, B.A. The pharmacology and clinical use of methotrexate. *N. Engl. J. Med.* **309**, 1094–1104 (1983).
- Schmiegelow, K. *et al.* Long-term results of NOPHO ALL-92 and ALL-2000 studies of childhood acute lymphoblastic leukemia. *Leukemia* **24**, 345–354 (2010).
- Toft, N. *et al.* Results of NOPHO ALL2008 treatment for patients aged 1–45 years with acute lymphoblastic leukemia. *Leukemia* **32**, 606–615 (2018).
- Widemann, B.C. *et al.* High-dose methotrexate-induced nephrotoxicity in patients with osteosarcoma. *Cancer* **100**, 2222–2232 (2004).
- Brown, P. *et al.* Pediatric acute lymphoblastic leukemia, version 2.2020, NCCN clinical practice guidelines in oncology. *J. Natl. Compr. Canc. Netw.* **18**, 81–112 (2020).
- Christensen, A.M. *et al.* Resumption of high-dose methotrexate after acute kidney injury and glucarpidase use in pediatric oncology patients. *Cancer* **118**, 4321–4330 (2012).
- Svahn, T. *et al.* Delayed elimination of high-dose methotrexate and use of carboxypeptidase G2 in pediatric patients during treatment



- for acute lymphoblastic leukemia. *Pediatr. Blood Cancer* **64**, e26395 (2017).
8. Widemann, B.C. *et al.* Glucarpidase, leucovorin, and thymidine for high-dose methotrexate-induced renal dysfunction: clinical and pharmacologic factors affecting outcome. *J. Clin. Oncol.* **28**, 3979 (2010).
  9. Krause, A.S. *et al.* Carboxypeptidase-G 2 rescue in cancer patients with delayed methotrexate elimination after high-dose methotrexate therapy. *Leukemia Lymphoma* **43**, 2139–2143 (2002).
  10. VORAXAZE. VORAXAZE® (glucarpidase) [package insert]. <[https://www.accessdata.fda.gov/drugsatfda\\_docs/label/2012/1253271bl.pdf](https://www.accessdata.fda.gov/drugsatfda_docs/label/2012/1253271bl.pdf)> (2012).
  11. Ramsey, L.B. *et al.* Consensus guideline for use of glucarpidase in patients with high-dose methotrexate induced acute kidney injury and delayed methotrexate clearance. *Oncologist* **23**, 52–61 (2018).
  12. Patterson, D.M. & Lee, S.M. Glucarpidase following high-dose methotrexate: update on development. *Expert Opin. Biol. Ther.* **10**, 105–111 (2010).
  13. Green, J.M. Glucarpidase to combat toxic levels of methotrexate in patients. *Ther. Clin. Risk Manag.* **8**, 403 (2012).
  14. Cavone, J.L., Yang, D. & Wang, A. Glucarpidase intervention for delayed methotrexate clearance. *Ann. Pharmacother.* **48**, 897–907 (2014).
  15. Mohty, M., Peyriere, H., Guinet, C., Hillaire-Buys, D., Blayac, J.-P. & Rossi, J.-F. Carboxypeptidase G2 rescue in delayed methotrexate elimination in renal failure. *Leukemia Lymphoma* **37**, 441–443 (2000).
  16. Widemann, B.C., Hetherington, M.L., Murphy, R.F., Balis, F.M. & Adamson, P.C. Carboxypeptidase-G2 rescue in a patient with high dose methotrexate-induced nephrotoxicity. *Cancer* **76**, 521–526 (1995).
  17. Zoubek, A. *et al.* Successful carboxypeptidase G2 rescue in delayed methotrexate elimination due to renal failure. *Pediatr. Hematol. Oncol.* **12**, 471–477 (1995).
  18. Treviño, L.R. *et al.* Germline genetic variation in an organic anion transporter polypeptide associated with methotrexate pharmacokinetics and clinical effects. *J. Clin. Oncol.* **27**, 5972 (2009).
  19. Watts, C.S. *et al.* Prophylactic trimethoprim-sulfamethoxazole does not affect pharmacokinetics or pharmacodynamics of methotrexate. *J. Pediatr. Hematol. Oncol.* **38**, 449–452 (2016).
  20. Pauley, J.L. *et al.* Between-course targeting of methotrexate exposure using pharmacokinetically guided dosage adjustments. *Cancer Chemother. Pharmacol.* **72**, 369–378 (2013).
  21. Rühls, H. *et al.* Population PK/PD model of homocysteine concentrations after high-dose methotrexate treatment in patients with acute lymphoblastic leukemia. *PLoS One* **7**, e46015 (2012).
  22. Panetta, J.C., Sparreboom, A., Pui, C.-H., Relling, M.V. & Evans, W.E. Modeling mechanisms of in vivo variability in methotrexate accumulation and folate pathway inhibition in acute lymphoblastic leukemia cells. *PLoS Comput. Biol.* **6**, e1001019-e (2010).
  23. Aumente, D., Buelga, D.S., Lukas, J.C., Gomez, P., Torres, A. & García, M.J. Population pharmacokinetics of high-dose methotrexate in children with acute lymphoblastic leukaemia. *Clin. Pharmacokinet.* **45**, 1227–1238 (2006).
  24. Albertioni, F. *et al.* Evaluation of clinical assays for measuring high-dose methotrexate in plasma. *Clin. Chem.* **42**, 39–44 (1996).
  25. Mould, D. & Upton, R.N. Basic concepts in population modeling, simulation, and model-based drug development—part 2: introduction to pharmacokinetic modeling methods. *CPT Pharmacometrics Syst. Pharmacol.* **2**, 1–14 (2013).
  26. Smith, R. *et al.* Population modelling by examples II. Proceedings of the Summer Computer Simulation Conference 1–8 (2016).
  27. Vinks, A.A. *et al.* Electronic health record-embedded decision support platform for morphine precision dosing in neonates. *Clin. Pharmacol. Ther.* **107**, 186–194 (2020).
  28. Kawakatsu, S. *et al.* Population pharmacokinetic analysis of high-dose methotrexate in pediatric and adult oncology patients. *Cancer Chemother. Pharmacol.* **84**, 1339–1348 (2019).
  29. Ramsey, L.B., Mizuno, T., Vinks, A.A. & O'Brien, M.M. Delayed methotrexate clearance in patients with acute lymphoblastic leukemia concurrently receiving dasatinib. *Pediatr. Blood Cancer* **66**, e27618 (2019).
  30. Byon, W. *et al.* Establishing best practices and guidance in population modeling: an experience with an internal population pharmacokinetic analysis guidance. *CPT Pharmacometrics Syst. Pharmacol.* **2**, 1–8 (2013).
  31. Bauer, R.J. NONMEM tutorial part I: description of commands and options, with simple examples of population analysis. *CPT Pharmacometrics Syst. Pharmacol.* **8**, 525–537 (2019).
  32. Barrett, J.S., Mondick, J.T., Narayan, M., Vijayakumar, K. & Vijayakumar, S. Integration of modeling and simulation into hospital-based decision support systems guiding pediatric pharmacotherapy. *BMC Med. Inform. Decis. Mak.* **8**, 6 (2008).
  33. Dombrowsky, E., Jayaraman, B., Narayan, M. & Barrett, J.S. Evaluating performance of a decision support system to improve methotrexate pharmacotherapy in children and young adults with cancer. *Ther. Drug Monit.* **33**, 99 (2011).
  34. Beechinor, R.J. *et al.* The population pharmacokinetics of high-dose methotrexate in infants with acute lymphoblastic leukemia highlight the need for bedside individualized dose adjustment: a report from the Children's Oncology Group. *Clin. Pharmacokinet.* **58**, 899–910 (2019).
  35. Zhang, C., Zhai, S., Yang, L., Wu, H., Zhang, J. & Ke, X. Population pharmacokinetic study of methotrexate in children with acute lymphoblastic leukemia. *Int. J. Clin. Pharmacol. Ther.* **48**, 11–21 (2010).
  36. Anderson, L.L., Collins, G.J., Ojima, Y. & Sullivan, R.D. A study of the distribution of methotrexate in human tissues and tumors. *Cancer Res.* **30**, 1344–1348 (1970).
  37. Chabner, B.A. *et al.* Polyglutamation of methotrexate. Is methotrexate a prodrug? *J. Clin. Investig.* **76**, 907–912 (1985).
  38. Mould, D., D'Haens, G. & Upton, R. Clinical decision support tools: the evolution of a revolution. *Clin. Pharmacol.* **99**, 405–418 (2016).
  39. Rousseau, A. & Marquet, P. Application of pharmacokinetic modelling to the routine therapeutic drug monitoring of anticancer drugs. *Fundam. Clin. Pharmacol.* **16**, 253–262 (2002).
  40. Dupuis, C. *et al.* High-dose methotrexate in adults with osteosarcoma: a population pharmacokinetics study and validation of a new limited sampling strategy. *Anticancer Drugs* **19**, 267–273 (2008).
  41. Ramsey, L.B. *et al.* Rare versus common variants in pharmacogenetics: SLC01B1 variation and methotrexate disposition. *Genome Res.* **22**, 1–8 (2012).
  42. Reiss, S.N., Buie, L.W., Adel, N., Goldman, D.A., Devlin, S.M. & Douer, D. Hypoalbuminemia is significantly associated with increased clearance time of high dose methotrexate in patients being treated for lymphoma or leukemia. *Ann. Hematol.* **95**, 2009–2015 (2016).
  43. Skärby, T. *et al.* High-dose methotrexate: on the relationship of methotrexate elimination time vs renal function and serum methotrexate levels in 1164 courses in 264 Swedish children with acute lymphoblastic leukaemia (ALL). *Cancer Chemother. Pharmacol.* **51**, 311–320 (2003).
  44. Wiczer, T., Dotson, E., Tuten, A., Phillips, G. & Maddocks, K. Evaluation of incidence and risk factors for high-dose methotrexate-induced nephrotoxicity. *J. Oncol. Pharm. Pract.* **22**, 430–436 (2016).
  45. Ramsey, L.B. *et al.* Genome-wide study of methotrexate clearance replicates SLC01B1. *Blood* **121**, 898–904 (2013).
  46. Radtke, S. *et al.* Germline genetic variations in methotrexate candidate genes are associated with pharmacokinetics, toxicity, and outcome in childhood acute lymphoblastic leukemia. *Blood* **121**, 5145–5153 (2013).
  47. Gaies, E. *et al.* Methotrexate side effects: review article. *J. Drug Metab. Toxicol.* **3**, 1–5 (2012).